Construction and Building Materials 259 (2020) 119805

Contents lists available at ScienceDirect

Construction and Building Materials

journal homepage: www.elsevier.com/locate/conbuildmat

Mechanical and self-healing behavior of low carbon engineered cementitious composites reinforced with PP-fibers

He Zhu [a], Duo Zhang [a], Tianyu Wang [a,b], Haoliang Wu [a], Victor C. Li [a,*]

[a] Department of Civil and Environmental Engineering, University of Michigan, Ann Arbor, MI 48109, USA
[b] College of Engineering, China University of Geosciences-Wuhan, Wuhan, Hubei Province, China

HIGHLIGHTS

- A sustainable ECC was developed using LC3 cement and PP fiber.
- The strain capacity of LC3-ECC (6%) is substantially higher than that of PP-ECC in the literature.
- LC3-ECC retains strength enhancement and no ductility loss after self-healing subsequent to 2% tensile straining.
- LC3-ECC reduces 61% of material cost, 45% of energy consumption, and 48% of carbon emission compared to M45-ECC.

ARTICLE INFO

Article history:
Received 11 January 2020
Received in revised form 29 May 2020
Accepted 1 June 2020

Keywords:
Engineered Cementitious Composites (ECC)
Limestone calcined clay cement (LC3)
Metakaolin
Limestone
Durability

ABSTRACT

While the ultrahigh tensile ductility and superior durability of Engineered Cementitious Composites (ECC) have been demonstrated, the relatively high energy and carbon intensity, as well as high material cost present potential impediments to broader ECC applications. The objective of this research is to develop a more sustainable and cost-effective ECC. The ordinary Portland cement (OPC) and the commonly used PVA fiber in conventional ECC were replaced by limestone calcined clay cement (LC3) and polypropylene (PP) fiber, respectively. The ECC compressive strength, tensile stress-strain relationship, and microcrack self-healing behavior were studied at three water to binder ratios (0.3, 0.2, 0.16). The novel LC3-PP-ECC showed a tensile strain capacity of greater than 6% and an intrinsically tight crack width below 82 μm when loaded to 1% tensile strain. Further, the LC3-PP-ECC demonstrated efficient recovery of the composite tensile ductility and ultimate tensile strength through self-healing. Compared to typical ECC made with OPC and PVA fiber, the material cost, embodied energy and carbon footprint of LC3-PP-ECC are reduced by 61%, 45%, and 48%, respectively. The superior mechanical properties and durability combined with the low environmental impact and cost for material production promote LC3-PP-ECC as a sustainable material for structural and non-structural applications.

1. Introduction

Concrete is the most widely used construction material, accounting for about 80% by weight of all engineering materials [1]. There are environmental concerns of concrete due to its use of Portland cement as a binder, which contributes 5–8% of the total anthropogenic CO_2 emissions [2]. The need for repeated repairs of concrete structures during its long service life (50–100 years) further adds to the concern of infrastructure sustainability. There is a clear demand for construction materials that combine high durability, low carbon and energy footprints, and high cost-effectiveness.

Engineered Cementitious Composites (ECC), a strain hardening fiber-reinforced cement-based composite extensively studied [1,3,4], is emerging in a variety of infrastructure applications [5–7]. Under tensile load, ECC suppresses brittle fracture in favor of tensile ductility several hundred times that of ordinary concrete [8]. During tensile strain-hardening, microcracks less than 100 μm are formed. The intrinsically tight crack width substantially enhances the structural durability of ECC [9]. However, for most ECC compositions previously studied, the high volumes of cement and polymeric fibers led to significant energy and carbon footprint, in addition to a high material production cost [9,10].

Supplementary cementitious materials (SCM) such as fly ash (FA), slag, and silica fume have been extensively used in ECC

* Corresponding author.
E-mail addresses: zhuhe14@tsinghua.org.cn (H. Zhu), duzhang@umich.edu (D. Zhang), tiawang@umich.edu (T. Wang), wuhaoliang@ust.hk (H. Wu), vcli@umich.edu (V.C. Li).

https://doi.org/10.1016/j.conbuildmat.2020.119805
0950-0618/

[1,6,9,11–13]. Their use can reduce the carbon and energy footprints. In particular, FA has been commonly adopted due to its broad availability and contribution to robust tensile ductility of ECC. The most studied M45-ECC, for example, uses FA in the amount of 1.2 times that of OPC. Despite this high SCM content, the CO_2 emission and embodied energy [13] remains high, 1.6 and 2.7 times that of conventional concrete. Hence, it is desirable to further lower the carbon and energy footprints of ECC by adopting a low carbon cement.

Calcined clay limestone cement (LC3) is an emerging alternative cement that mitigates the environmental impacts for concrete production [14,15]. Compared to ordinary Portland cement (OPC), LC3 has been proven to reduce the binder carbon emissions by 20%–35% [2,16], the energy consumption by 22% [17], and the material costs by 15–25% [2,16]. The abundance of clay and limestone worldwide assures supply chain continuity [14]. Studies show that the mixture LC3-50 (50% clinker, 30% calcined clay, 15% limestone, and 5% gypsum) gives comparable mechanical properties with OPC in concrete or mortar [18]. LC3 cement paste possesses a finer pore structure than OPC paste. Additionally, concrete durability can be improved using LC3 with respect to chloride ingress, alkali-silica reaction, water sorptivity, gas permeability, and carbonation [18,19]. LC3 cement could be produced in existing plants, and the industrial scalability has been demonstrated in India [20] and Cuba [16].

Though LC3 cement has not been used in ECC compositions, the addition of limestone (LS) or metakaolin (MK) separately in ECC has attracted attention. Turk [21] suggested that the replacement of sand with limestone improved the tensile ductility and durability of ECC. Zhou [12] found that with increasing limestone power content, the ductility of ECC first increased and then decreased. Siad [22] suggested that LS increased the deflection-hardening of ECC. MK improved the fiber distribution performance of ECC and increased the ductility [23,24]. Zheng [25] found that a combination of 90% cement, 5% MK, and 5% LS increased the tensile ductility and decreased the crack width, while Özbay suggested that using MK resulted in larger crack widths [26]. Thus, the viability of ECC using LC3 appears feasible and warrants further research.

High-tenacity polypropylene (PP) fiber was studied as an alternative to Polyvinyl Alcohol (PVA) fiber because of its lower cost and energy intensity [3]. PP ECC was found to have ductility (3% strain capacity) comparable to that of PVA ECC [27]. ECC with hybrid PVA and PP fibers showed improved ductility with lower strength [28]. Though the average crack width of PP-ECC (134 μm) is larger than PVA ECC (50 μm) [3,24], PP fiber remains a potential substitute for PVA fiber for developing sustainable ECC, under the assumption that the crack width could be reduced. There is a need to investigate the feasibility of PP fiber working with the LC3 cement matrix, especially for assuring robust tensile strain-hardening behavior and tight crack width.

The objective of this research is to develop a sustainable ECC using LC3 cement and PP fiber. The sustainable LC3-ECC features lower embodied energy and carbon, and lower cost than those of conventional PVA-ECC, while retaining high tensile strain capacity, low crack width, and robust self-healing ability. To develop LC3 based ECC for different strength applications, three water to binder ratios were prepared. The composite compressive strength, tensile properties, crack bridging behavior, self-healing, and environmental impact were investigated and reported here.

2. Experimental program

2.1. Materials and mix proportions

Type I ordinary Portland cement (OPC, Lafarge Holcim Cement Co., MI, USA) conforming to ASTM C150 [29] was used. Fly ash (FA, Boral Material Technologies Inc) was adopted as the SCM. The metakaolin (MK) and limestone (LS) are commercially available as Sikacrete® M-100 (Sika Corporation, USA) and Snowhite® 12–PT (Omya Canada Inc). Superplasticizer (SP, MasterGlenium 7920, BASF) was adopted as a water reducer. The PP fiber Brasilit (from Saint-Gobain Brazil) has 12 μm diameter, 10 mm length, 6 GPa Young's modulus, and 850 MPa tensile strength.

The chemical compositions and X-ray diffraction patterns of the OPC and LC3 ingredients (MK, LS) can be found in Table 1 and Fig. 1, respectively, while their particle size distributions can be found in Fig. 2. Scanning electron microscope (SEM) images of these ingredients can be found in [30–32]. The LC3 used in this study is blended with 55% OPC, 30% MK, and 15% LS. The XRD results (Fig. 1) show that the main mineral of LS was calcite, while MK presents a hump pattern due to its highly amorphous property. This differs from the XRD result of the commercially premixed limestone-calcined clay (LCC) [33] that shows impurities besides MK and LS.

Table 2 lists the mix proportions in this study, in which three water/binder ratios (W/B = 0.3, 0.2, and 0.16) were designed for different grades of composite strength [5,34]. LC3 cement comprising 55% OPC, 30% MK, and 15% LS was used for developing sustainable ECC, and conventional OPC-ECC was prepared as the control.

To prepare specimens, all dry ingredients (OPC, MK, LS, and FA) were mixed in a 4-liter mortar mixer at 100 rpm for 10 min. The mixing time is longer than that for conventional OPC-ECC (5 min) to ensure sufficient blending of LC3 cement. The water premixed with SP was then added to the dry ingredients which were further mixed for 6 min at 100 rpm. The composite mixture was finalized by adding PP fibers and mixing at 150 rpm for an additional 6 min.

2.2. Test methods

2.2.1. Mechanical performance tests

The fresh mixtures were cast into 50 × 50 × 50 mm^3 cubes and dogbone-shaped molds. The geometry of the dogbone-shaped specimen is shown in Fig. 3 with a thickness of 13 mm. After 28 days curing in air (20 ± 3 °C, 40 ± 5% RH), cube specimens were tested in compression following ASTM C109 [36]. Uniaxial tension test was performed with the dogbone-shaped specimens (following [3,37]) on an Instron servo-hydraulic system at a rate of 0.5 mm/min. The deformation was measured by two linear variable displacement transducers (LVDT) with an 80 mm gauge length.

During the tensile test, the crack numbers were recorded manually when the dogbone specimen reached 1%, 2%, and 3% strain levels. Then the average crack width (CW) was measured by dividing the tensile elongation by crack number [38], assuming negligibly small elastic deformation of the material between the subparallel cracks.

To prepare a single-notch tensile specimen, a reduced section (Fig. 3 insert) was introduced into a dogbone-shaped specimen with a diamond saw (0.5 mm thickness). During tensioning, fiber bridging stress (the measured tensile load divided by the remaining ligament cross-sectional area after notching) was obtained as a function of the crack opening monitored by two LVDTs attached to the specimen [4].

Three specimens of each Mixture ID in Table 2 were tested for compressive strength, uniaxial tension test, and single crack test, and their average values were set as the representative results.

2.2.2. Self–healing test

Prior studies demonstrated that the intrinsically tight crack width together with the presence of unhydrated cement grains promoted the autogenous healing of ECC [39]. However, with the

Table 1
Chemical compositions of OPC, MK, and FA.

Material	CaO	SiO_2	Al_2O_3	Fe_2O_3	SO_3	MgO	K_2O	TiO_2	MnO	P_2O_5
OPC	67.5	17.7	4.2	3.7	3.6	2.0	0.6	0.3	0.1	0.1
MK	0.0	50.8	46.6	0.5	0.1	0.0	0.3	1.7	0.0	0.0
FA	3.4	52.2	22.2	13.5	2.2	0.9	2.6	1.0	0.0	0.1

Note: LS is a highly pure $CaCO_3$ powder, and the main composition is CaO (Fig. 1).

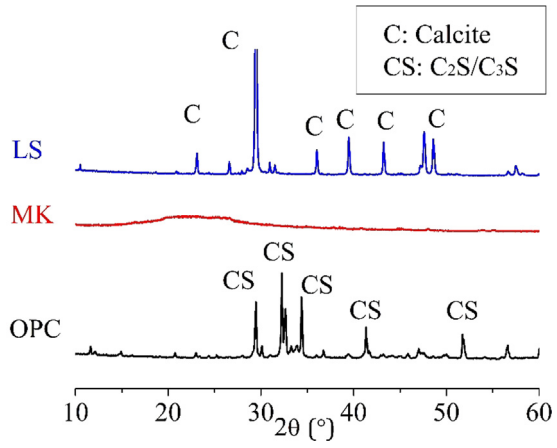

Fig. 1. X-ray Diffraction analysis of OPC, MK, and LS.

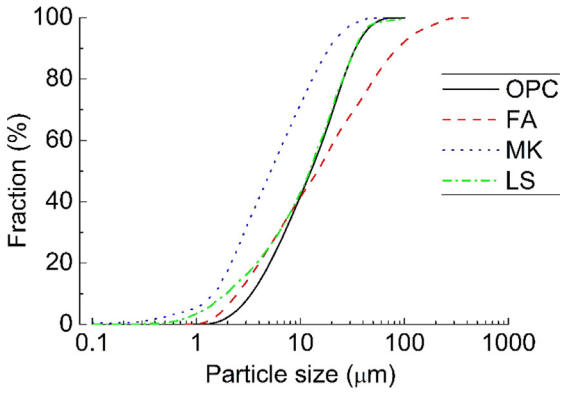

Fig. 2. Particle size distribution of binder ingredients (OPC, FA, MK, and LS).

replacement of OPC by LC3, LC3-ECC is expected to have a lower amount of unhydrated cement. Further, the crack width performance is unknown. To evaluate the self-healing performance of LC3-ECC, the resonant frequency and tensile performance of healed specimens were measured and analyzed.

After 28 days curing in air (20 ± 3 °C, 40 ± 5% RH), dogbone-shaped specimens of both W03-LC3 and W03-OPC were

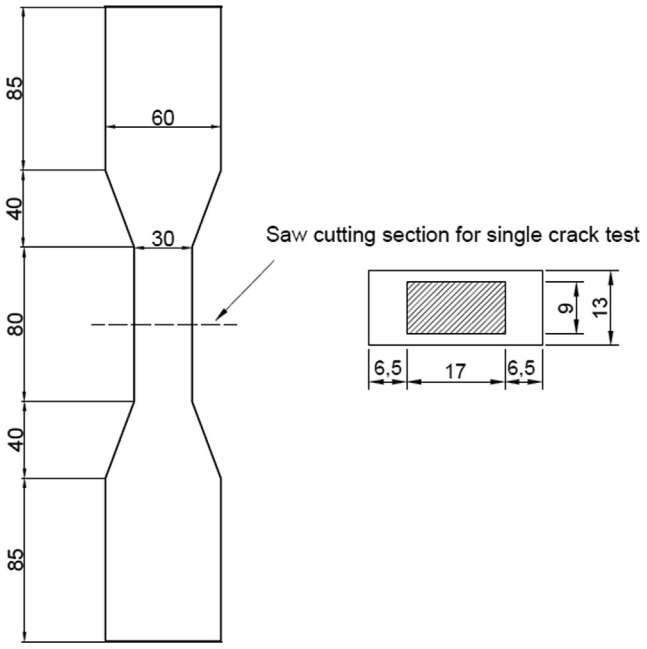

Fig. 3. Dimensions of the dogbone-shaped ECC specimen for uniaxial tension and single-crack test. (Unit: mm). For the single-crack test, specimens were pre-notched as shown on the right.

pre-tensioned to 1% and 2% strain level. The pre-cracked specimens were then exposed to a wet-dry cycles comprising 24-h water immersion and 24-h air drying. Three specimens were tested in each batch of W03-LC3-1%, W03-LC3-2%, W03-OPC-1%, and W03-OPC-2%. After 7 wet-dry cycles, the pre-cracked specimens were tested under uniaxial tension until failure. The tensile strength and strain capacity were used to evaluate the self-healing performance.

The resonant frequency (RF) technique has been proven to be a good gauge to evaluate the material damage and the degree of healing [39–41]. Fig. 4 depicts the protocol of RF measurement according to the ASTM C215 [42]. The dogbone-shaped specimen was placed on a rubber plate and impacted by a needle hammer. The sensor monitored the signals generated by impacting, and then the RF was calculated by the resonance tester (Olson, model RT-1).

Table 2
Mixture proportions of ECC (kg/m^3).

Mixture ID	OPC	MK	LS	FA	PP[a]	Water	SP	$\bar{d}$[b]	Density [c]
W03-OPC	490	0	0	1078	2%	470	2.00	190	1905
W02-OPC	490	0	0	1078	2%	314	8.50	178	2051
W16-OPC	490	0	0	1078	2%	251	16.4	170	2105
W03-LC3	270	147	74	1078	2%	470	4.00	185	1790
W02-LC3	270	147	74	1078	2%	314	13.60	173	2005
W16-LC3	270	147	74	1078	2%	251	22.70	165	2035

[a] Volume fraction.
[b] Average flow diameter (unit: mm) tested per ASTM C1437 [35]. The fresh property in this work is consistent with [33], assuring the good fiber dispersion.
[c] Bulk density [33]. Specimens were measured after 28 days curing in air.

Both the virgin specimens and cracked specimens were measured before each wet cycle.

A "*Normalized RF*" is proposed to measure the RF recovery degree and is calculated by the following equation:

$$Normalized\ \ RF = \frac{RF_{cracked}}{RF_{virgin}} \times 100\% \quad (1)$$

where $RF_{cracked}$ is the RF of the pre-loaded specimen, which varies with the number of wet-dry cycles. RF_{virgin} is the RF of the specimen before pre-cracking.

3. Results and discussions

3.1. Compressive strength

The compressive strength of OPC-ECC and LC3-ECC at 28d is presented in Fig. 5. When the W/B ratio decreases from 0.3 to 0.16, the compressive strength of LC3-ECC increases from 20 to 47.3 MPa, which is comparable to the compressive strength of high volume limestone calcined clay (LCC) ECC [33]. Similarly, the compressive strength of OPC-ECC increases from 28.6 to 53.6 MPa. Though the composite compressive strength is lower for LC3-ECC than OPC-ECC at the same W/B ratio, the strength difference becomes smaller as W/B decreases. The strength ratio of LC3-ECC to OPC-ECC is 70% at W/B of 0.3, but increases to 86% at W/B of 0.16.

The water for hydration affects the composite strength. The low W/B ratio (0.2, 0.16), along with the air curing condition (rather than in a 100%RH chamber) may lead to insufficient moisture for complete hydration of cement. However, Avert [43] attests that the internal relative humidity of the specimen decreases less in the LC3 mixture than that in the OPC mixture. In other words, less water is consumed in LC3 cement than in OPC. Since LC3 contains

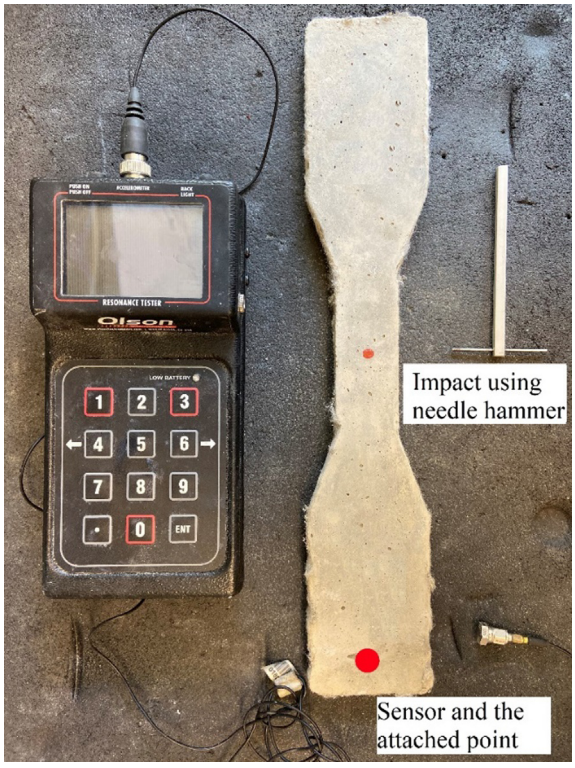

Fig. 4. Resonance frequency test set-up.

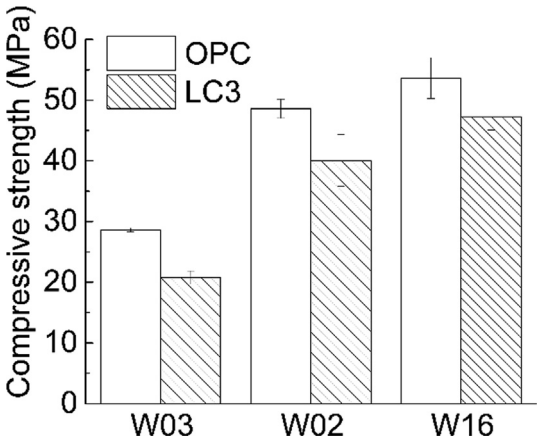

Fig. 5. Compressive strength of OPC-ECC and LC3-ECC at 28d.

55% OPC, 30% MK, and 15% LS, the effective water to cement ratio of LC3 is nearly twice that of OPC [44]. Hence, despite the low W/B ratio (0.16) and air curing, LC3-ECC attains a higher degree of hydration than OPC-ECC, leading to a smaller strength difference between LC3-ECC and OPC-ECC at W/B of 0.16.

Distinct from the lower strength of ECC with LC3 as the binder, concrete mixed with LC3 cement does not show obvious strength reduction compared with the OPC-concrete [14,18,19]. Though LC3 cement (comprising 55%OPC, 30%MK, 30%LS) has lower OPC cement, the pozzolanic effect of MK contributes to the strength increase by reacting with the calcium hydroxide (CH) [14,45] produced by OPC hydration [46]. Thus, though the cement volume is reduced, the compressive strength of LC3 based concrete is comparable to that of OPC based concrete. However, due to the large volume of FA used in the ECC mixture, the binder of the LC3-ECC mixture only contains 17% of OPC, much lower than the ratio in conventional concrete/mortar [14,18,19]. Hence, the CH quantity generated by OPC hydration in the LC3-ECC mixture is less than that in the concrete mixture, limiting the pozzolanic reaction of MK and decreasing the strength contribution. Another reason is the competitive consumption of CH between FA and MK [47]. The weight of FA is more than 7 times of MK in ECC mixtures as shown in Table 1, so FA would consume more CH than MK. The insufficient CH reacting with MK further impedes the strength increase.

3.2. Tensile performance

Fig. 6 depicts the uniaxial tensile stress-strain curves of OPC-ECC and LC3-ECC. The stress corresponding to the first crack is named "first crack strength (f_0)"; The peak stress approaching specimen failure is named "ultimate tensile strength (f_u)", and the corresponding strain is defined as "tensile strain capacity (ε_t)". Table 3 lists the characteristic values of tensile performance for the mixtures in this study, where σ_0 is the maximum fiber bridging stress obtained from single-crack tests described in Section 3.3.

Similar to the trend of compressive strength, the first crack tensile strength and ultimate tensile strength of LC3-ECC are lower than those of OPC-ECC at the same W/B ratio. The tensile strength data scatter is higher for OPC-ECC than that for LC3-ECC (Fig. 6). The ultimate tensile strength is determined by maximum fiber-bridging stress, which is affected by fiber dispersion [48]. The increased viscosity of the matrix of LC3 cement promotes fiber dis-

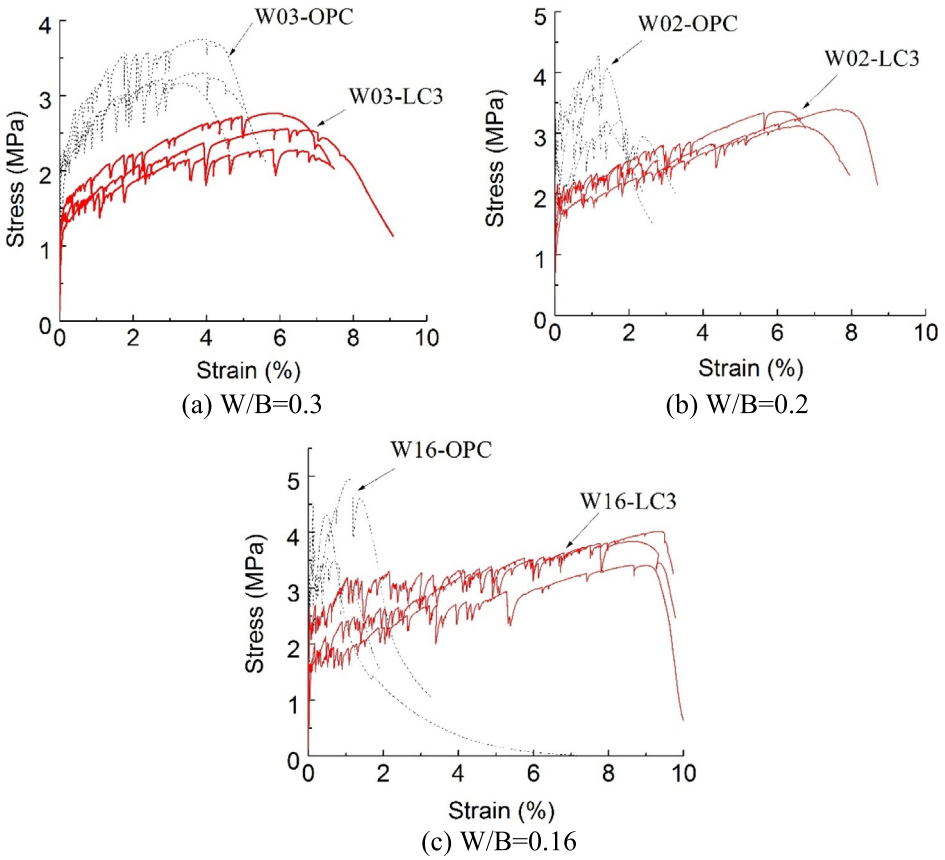

Fig. 6. Tensile stress-strain relationships of OPC-ECC and LC3-ECC.

Table 3
Tensile properties of OPC-ECC and LC3-ECC.

Mixture	f_0 (MPa)	f_u (MPa)	σ_0 (MPa)	ε_t (%)	σ_0/f_0
W03-OPC	2.1	3.4	3.6	3.7	1.7
W02-OPC	2.6	4.0	4.5	1.1	1.7
W16-OPC	3.9	4.8	5.3	0.6	1.4
W03-LC3	1.4	2.5	3.2	6.0	2.3
W02-LC3	1.7	3.3	4.4	7.1	2.6
W16-LC3	2.0	3.8	5.3	8.9	2.7

persion effect [49], resulting in a smaller scatter of the ultimate tensile strength of LC3-ECC.

For W03-OPC, the tensile strain capacity is 3.7% which is comparable to other ECC mixtures with PP fibers [3]. However, the tensile strain capacity decreases dramatically to only 0.6% at a W/B ratio of 0.16. Fig. 7 (a–c) shows that smaller crack numbers are observed as the W/B ratio decreases, which accounts for the ductility reduction. However, the strain capacity of LC3-ECC is higher than that of OPC-ECC. LC3-ECC reveals a robust strain hardening behavior at three W/B ratios (0.16, 0.20, and 0.30). In contrast to OPC-ECC, the tensile strain capacity of W03-LC3 is 6.0% and increases to 8.9% for W16-LC3. This is substantially higher than the tensile strain capacity reported for LCC-ECC (0.57–1.58%) [33]. The ultimate tensile strength (2.5–3.8 MPa) meets the tensile strength requirement of common concrete applications.

The crack width (CW) represents one of the limitations of ECC reinforced with PP fibers. The CW (86.7–144.0 μm) of W03-OPC and W02-OPC in Table 4 is consistent with the published CW data on PP-ECC (95–151 μm) [3]. However, the CW is much larger than that of PVA-ECC (50–80 μm) [1]. Compared to OPC-ECC, ECC mixed with LC3 reduces the CW. At tensile strains of 1–3%, the CW of W03-LC3 is smaller than that of W03-OPC. W02-LC3 and W16-LC3 further reduce the CW to approximately 60–85 μm, which is comparable with that of typical PVA-ECC (50–80 μm) [1].

Table 4 shows that the crack spacing (dividing the gauge length by the crack number) becomes smaller as the strain increases, as expected. The smaller crack spacing of LC3-ECC represents a higher density of microcracks compared to that of OPC-ECC. When W/B decreases from 0.3 to 0.16, the crack spacing also decreases from 8.2 to 6.0 mm (at 1% strain), 5.3 to 4.0 mm (at 2% strain), and 4.3 to 2.8 mm (at 3% strain). LC3-ECC shows saturated multiple cracks and denser cracks (Fig. 7), while the crack numbers of OPC-ECC are significantly less than LC3-ECC.

The composite tensile strain capacity and crack width control ability were enhanced by the use of LC3 in place of OPC for producing PP-ECC [23,50–55]. The enhanced ductility and tight crack width are anticipated to improve the service life of ECC. Based on a steel corrosion model [56], the service life of a 3.0% strain capacity ECC was 60 years. A 6.0% strain capacity would imply a service life more than 120 years. LC3-ECC has advantages of increasing the

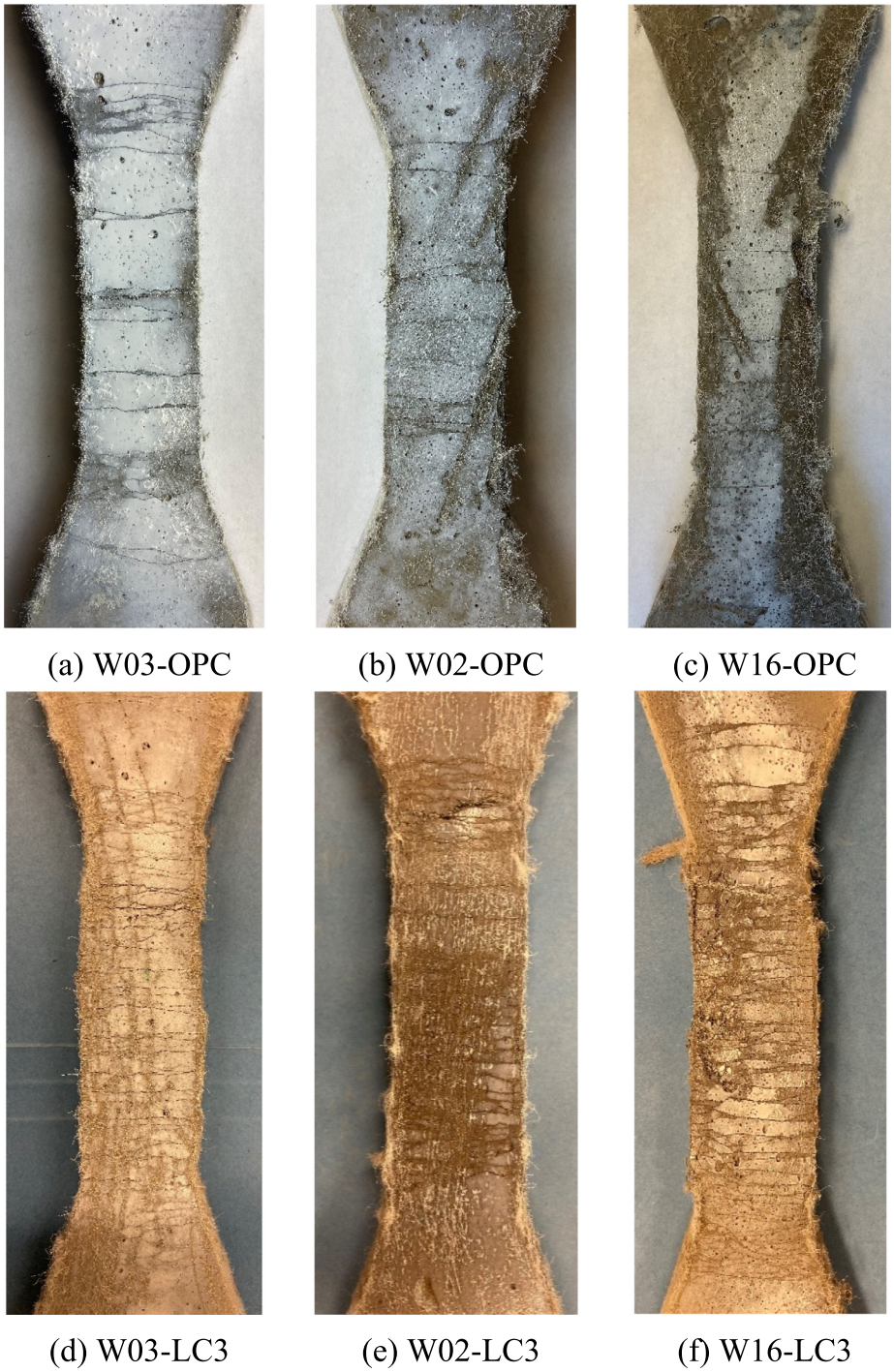

Fig. 7. Crack patterns of uniaxial tension specimens.

Table 4
Average crack width and spacing at tensile strains of 1%–3%.

Mixture	Crack width (μm)			Crack spacing (mm)		
	1%	2%	3%	1%	2%	3%
W03-OPC	86.7	115.5	144.0	8.7	5.8	4.8
W02-OPC	101.2	–	–	10.1	–	–
W16-OPC	–	–	–	–	–	–
W03-LC3	81.6	105.7	127.8	8.2	5.3	4.3
W02-LC3	68.8	82.7	86.5	6.9	4.1	2.9
W16-LC3	60.0	80.7	83.8	6.0	4.0	2.8

service life and decreasing the repair/maintenance frequency, improving sustainability due to lower long-term material cost, and carbon and energy footprints.

3.3. Single-crack test results

The fiber bridging stress (σ_0) and crack opening results are shown in Fig. 8 and listed in Table 3. The maximum fiber bridging stress of OPC-ECC increases from 3.6 MPa to 5.3 MPa when W/B decreases from 0.3 to 0.16. σ_0 of LC3-ECC ranges from 3.2 MPa to 5.3 MPa. Though LC3-ECC has a lower compressive strength than OPC-ECC, the maximum fiber bridging stress is nearly identical at the same W/B ratio. The compressive strength is determined by matrix while the fiber bridging stress is governed by fiber-matrix bonding strength and the amount of fiber bridging in the crack section. In principle, the maximum bridging stress σ_0 and the composite ultimate tensile strength f_u should be identical. In practice, however, the f_u will be lower than $\sigma_0$since the composite will fail by localizing fracture on the plane with the lowest amount of fiber when fiber dispersion is non-uniform. This observation is reflected by the lower values of f_u compared to σ_0 in Table 3 for all mixes.

A lower W/B ratio may be expected to reduce the porosity of the matrix. The densified matrix increases the strength and results in a higher fiber-matrix interfacial frictional bond, which further increases the fiber bridging stress, as revealed in Fig. 8 and Table 3. To attain a robust strain-hardening performance, a larger margin between fiber bridging stress and the first crack strength is preferred. The strength index of σ_0/f_0 was proposed as 2 for the PP-ECC system to attain multiple cracking [27]. As listed in Table 3, σ_0/f_0 of OPC-ECC decreases from 1.7 to 1.4 when W/B decreases from 0.3 to 0.16. The narrowing margin accounts for the ductility loss of W16-OPC due to fewer cracks, which is consistent with the results in [57]. In contrast to OPC-ECC, the decreased W/B ratio of LC3-ECC results in an increased σ_0/f_0 from 2.3 to 2.7. The increased margin of LC3-ECC promotes W02-LC3 and W16-LC3 multiple cracking, consistent with the increased ductility in Fig. 6. According to the micromechanical fiber bridging model [3,4], a higher fiber-matrix interfacial frictional bond leads to a smaller crack opening (at the same stress level), which is also revealed in Fig. 8. The bridging model results can account for the observed smaller CW of W16-LC3 than W03-LC3.

3.4. Self-healing performance

3.4.1. Resonant frequency (RF) recovery of LC3-ECC and OPC-ECC

Fig. 9 plots the normalized RF of OPC and LC3 after healing. After 1% pre-cracking strain, the RF loss is comparable for W03-OPC (80%) and W03-LC3 (75%). However, W03-OPC-2% has a larger RF reduction to 55% than W03-LC3-2% (73%) because of its larger crack width. The RF of W03-OPC increases continuously during the 7 wet-dry cycles, while most healing of W03-LC3 occurs in the first 3 cycles. Note that it is possible for normalized RF to be higher than 100% due to continued hydration of the composite during the wet-dry cycles. According to [39,41,58], continued hydration of unhydrated cementitious materials and carbonation of calcium hydroxide are the dominant autogenous healing mechanisms of ECC. Because the unhydrated cementitious material of W03-LC3 is less than W03-OPC, the RF for W03-LC3 shows negligible recovery after the third cycle.

The healing effect is mainly determined by the unhydrated cement and crack width (CW). With respect to 1% pre-cracking strain, though the CW of W03-LC3 (81.6 μm) was slightly lower than W03-LC3 (86.7 μm), the RF recovery of W03-LC3 was smaller than W03-OPC-ECC due to a relatively high content of unhydrated cement in W03-OPC. However, at a 2% pre-cracking strain, the RF recovery of W03-LC3 (90%) was higher than that of W03-OPC (86%). Large CW hinders autogenous healing, and no healing recovery would occur when the CW exceeds the threshold. Though the maximum allowable CW varies between mixtures and healing environment, it was proposed to control the crack width under 150 μm, and possibly 50 μm [39,59]. The smaller CW of W03-LC3 demonstrates the slightly higher RF recovery than W03-OPC.

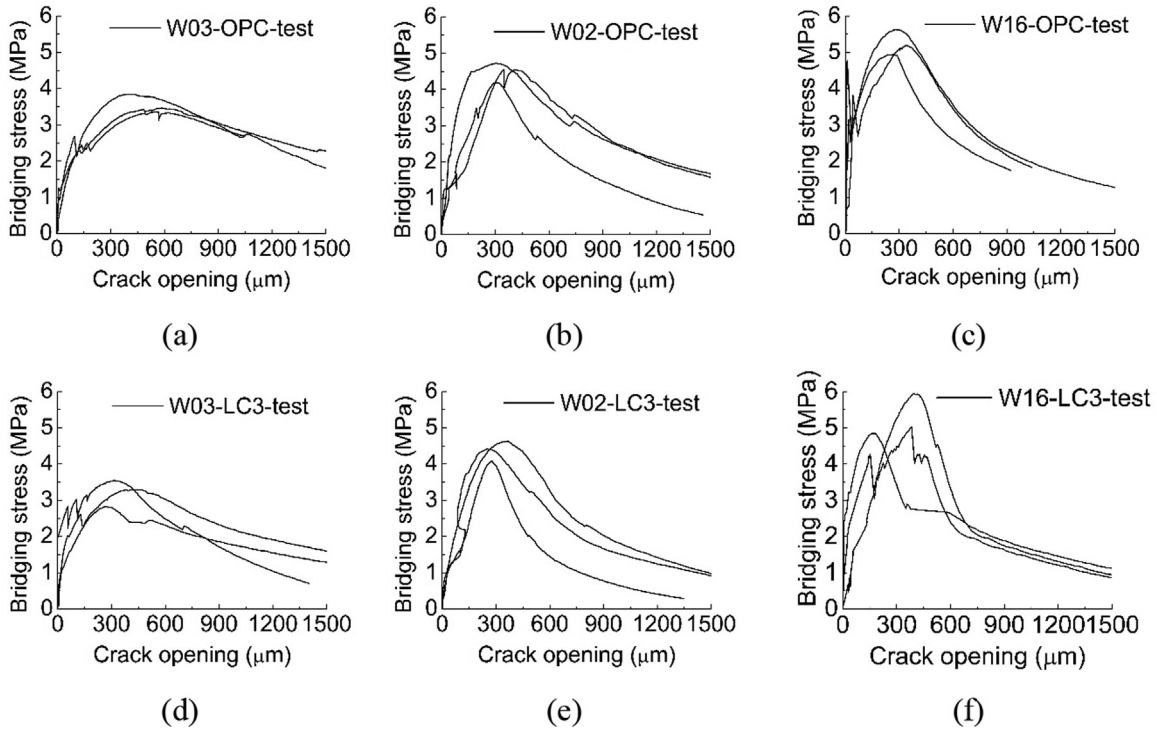

Fig. 8. Fiber bridging stress and crack opening relationships from single-crack tests.

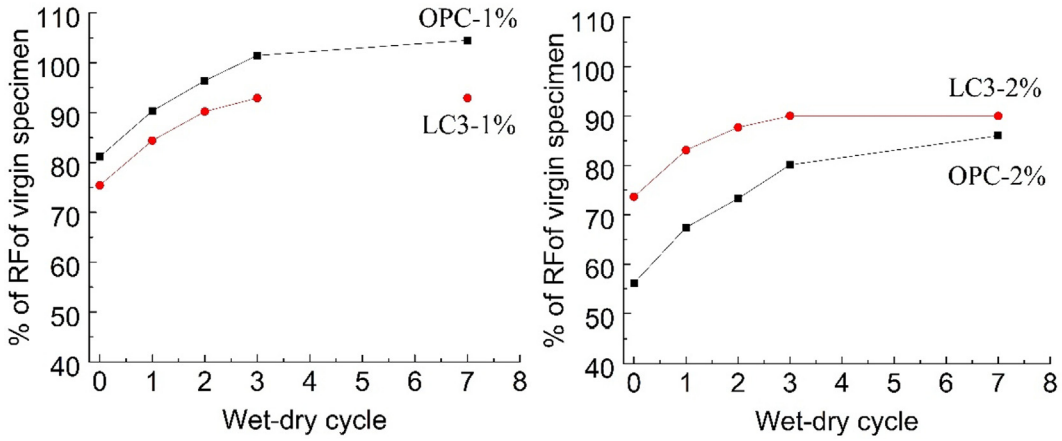

Fig. 9. Normalized RF of OPC and LC3 based ECC at 1% and 2% preload strain levels.

Table 5
Ultimate strength and strain capacity after 7 wet-dry cycles.

Pre-crack strain level	W03-OPC		W03-LC3	
	f_u (MPa)	ε_t (με)	f_u (MPa)	ε_t (με)
0%	3.4	3.7	2.5	6.0
1%	4.5	3.7	3.4	5.6
2%	4.4	2.8	3.5	5.6

3.4.2. Tensile performance recovery of LC3-ECC and OPC-ECC

After 7 wet-dry cycles, the pre-cracked specimens were re-tested in direct tension. Table 5 lists the ultimate strength and strain capacity after healing. Fig. 10 plots the comparative stress-strain response at all pre-cracking strain levels after 7 wet-dry cycles. Because the continued hydration increases the fiber/matrix interfacial frictional bond [59,60], the maximum bridging stress is increased, resulting in a higher ultimate tensile strength for the self-healed specimen than the virgin specimen at 28d.

The W03-LC3 shows significant advantages in post-healed tensile strain capacity. The W03-LC3 maintained 5.6% tensile strain capacity, 94% of virgin specimens, after experiencing 2% pre-cracking strain and 7 wet-dry cycles. The W03-OPC retained 2.8% tensile strain capacity, lower than the strain capacity of the virgin specimens. The high strain capacity and the tight crack width of the virgin W03-LC3 both contribute to the strain capacity after healing.

The healing degree of cracks is affected by crack width. Figs. 11 and 12 present the images of cracks before and after the wet-dry exposure. Both W03-LC3 and W03-OPC reveal full healing for crack width below 30 μm, partial recovery for crack width between 30 and 50 μm, and negligible healing for crack width larger than 50 μm, consistent with observations in previous studies [39,59].

The majority of concrete structure deformation due to shrinkage, thermal, and mechanical loading is expected to be substantially below 2% strain. The self-healing results indicated that the novel LC3-ECC was able to retain a 5.6% tensile strain capacity at 2% strain level after self-healing which secures a good structural durability.

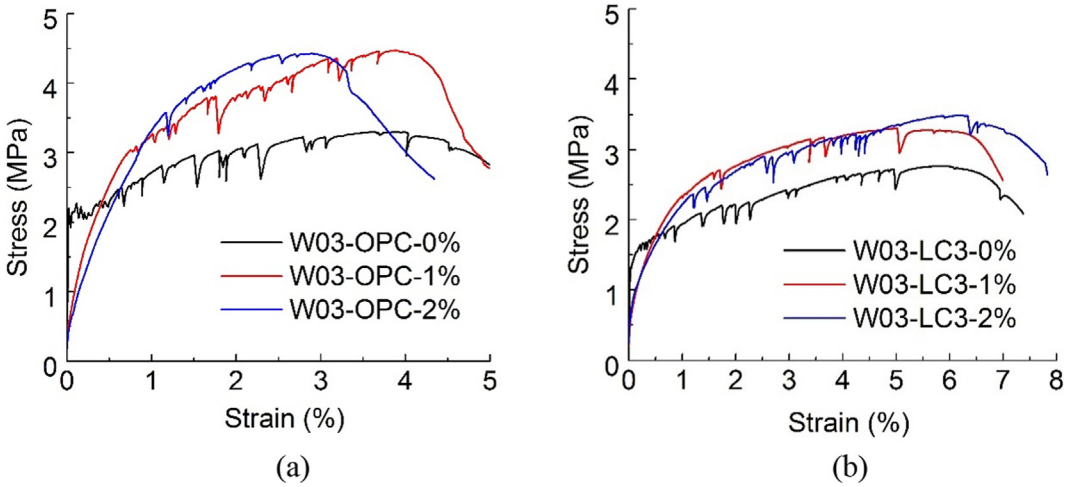

Fig. 10. Stress-strain response of pre-cracked specimens (a) OPC based, and (b) LC3 based ECC after 7 wet-dry cycles.

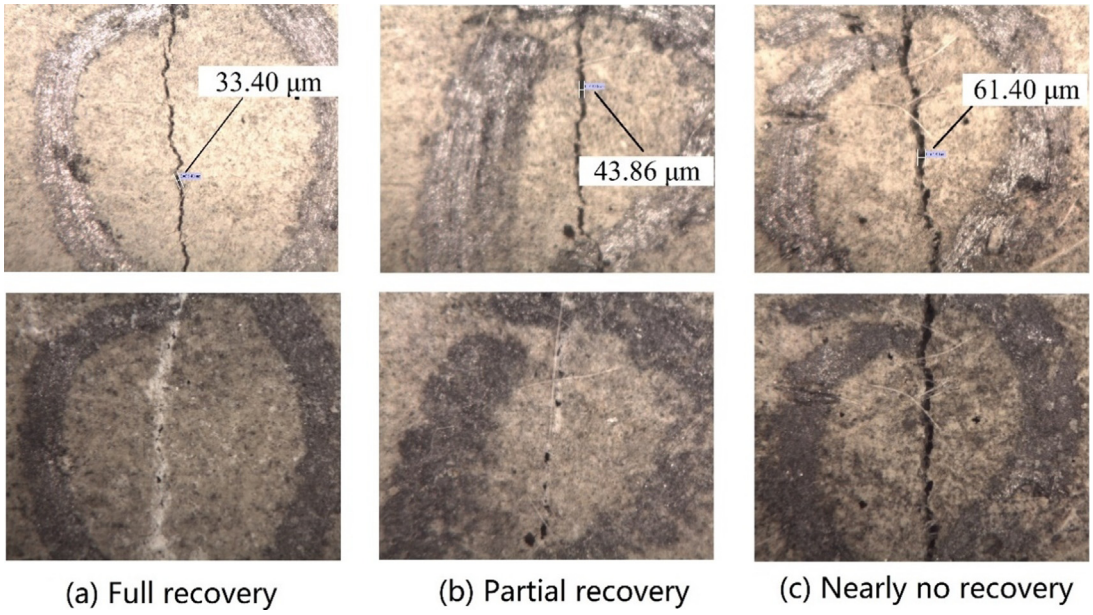

Fig. 11. The appearance of cracks of OPC-ECC before (top row) and after healing (bottom row) (Measured by a HIROX microscope, Model: CX-5040RZ).

3.5. Sustainability of LC3-ECC

To evaluate the sustainability of LC3-ECC, Material Sustainability Indicators (MSI) were adopted from the perspective of embodied energy, carbon footprint, and material cost [9,10]. Embodied energy [61] is the total energy required to manufacture the material, and carbon footprint [62] represents the total amount of greenhouse gases (CO_2 herein) associated with material production, including the extraction, processing, fuel combustion, and transportation, etc. The MSI data of ECC ingredients listed in Table 6 are the average estimated values from the literatures. Figs. 13–15 plots the total MSI for LC3-ECC and OPC-ECC. The results are based on W03-LC3 and W03-OPC with PP fiber. The MSI of conventional concrete and M45-PVA-ECC [37] were adopted as the benchmark for LC3-PP-ECC.

The M45-ECC matrix is typically formulated with OPC (583 kg/m^3), FA (700 kg/m^3), silica sand (467 kg/m^3), and water (298 kg/m^3) with the addition of SP (0.015 kg/m^3) for achieving adequate workability. PVA fiber is normally added at 2 vol% to form ECC [37]. At the standard 28 days, M45-ECC has a 40 MPa compressive strength, 4.5 MPa ultimate tensile strength, and 3% tensile strain capacity. Due to the relatively high cement dosage, the carbon footprint of M45-ECC is nearly twice that of typical concrete. By introducing LC3 in place of OPC, the composite carbon footprint was lowered to 90% of concrete and 67% of the ECC M45 due to the substantial reduction of OPC usage. The embodied energy of

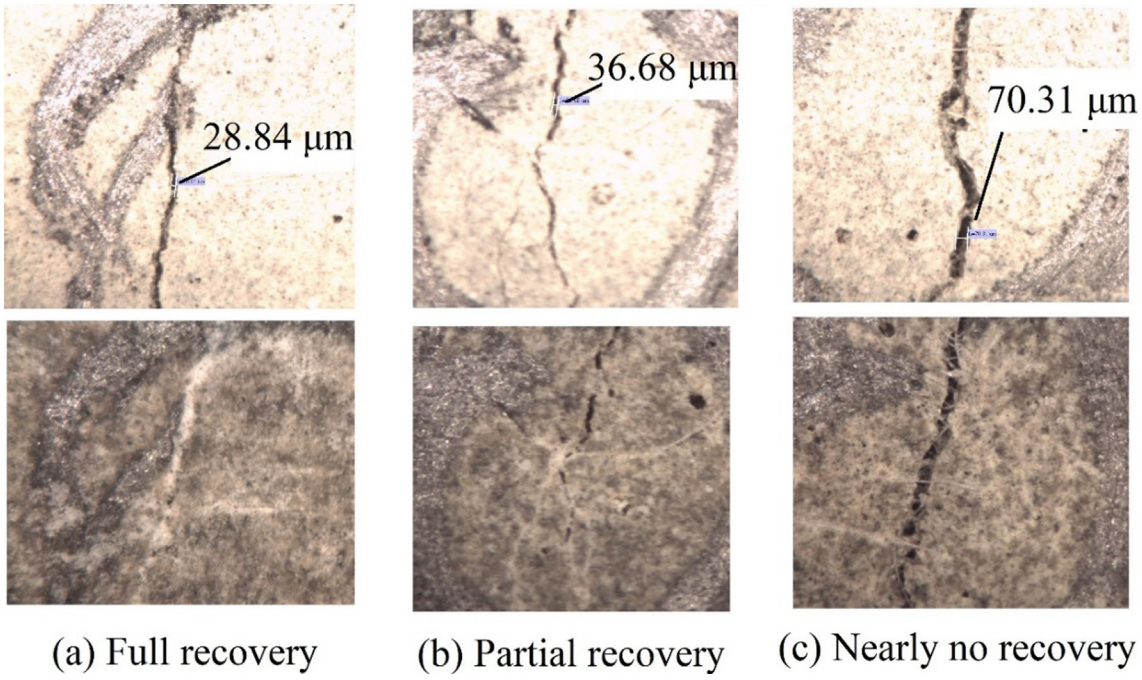

Fig. 12. The appearance of cracks of LC3-ECC before (top row) and after healing (bottom row) (Measured by a HIROX microscope, Model: CX-5040RZ).

Table 6
The embodied energy, carbon footprint, and material cost of the ECC ingredients.

MSI	LC3	OPC	FA	PP	PVA	Sand	SP	water
Energy (GJ/ton)	4[a]	5.5[b]	0	77.24[c]	101[b]	0.067[b]	35[b]	0
CO_2 (kg/ton)	560[a]	900[b]	0	3100[d]	3400[f]	23.3[b]	1667[b]	0
Cost ($/ton)	40.3[a]	48[b]	25.6[b]	6335[e]	12670[b]	63.9[b]	1211[b]	1.5

[a] Data from [16].
[b] Data from [1,37].
[c] Data from [63].
[d] Data from [53].
[e] Cost was estimated as half of PVA fiber [3,27].
[f] Data from [6].

ECC M45 is higher than that of conventional concrete due to the incorporation of PVA fibers. In particular, the embodied energy of M45-ECC made with PVA fiber was 2.4 times that of conventional concrete while over half of the embodied energy was attributed to PVA fiber. By utilizing PP fiber in place of PVA, OPC-PP-ECC reduces embodied energy down to 150% of concrete. The adoption of LC3 cement in place of OPC further cuts its embodied energy to 129% of concrete and 55% that of M45-ECC.

High volume limestone calcined-clay (HVLCC) was used as an alternative binder to FA in ECC [33]. The mixture L80S20W40 reported in [33] was chosen for carbon and energy footprint comparison since the mechanical performance and the cement dosage are comparable to the W03-OPC version in this study. The carbon footprint of HVLCC ECC is approximately 60% of M45-PVA and 80% of OPC-PP (Fig. 13) due to the low carbon contribution of LCC. However, the carbon footprint of HVLCC ECC is higher than the developed LC3-PP ECC in this study. For the embodied energy (Fig. 14), HVLCC ECC does not show an advantage over M45-ECC because of the higher energy of HVLCC than FA. Since LC3-PP ECC adopted LC3 cement as well as FA as the binder system, it emits only 74% of CO_2 and consumes 50% of energy of HVLCC ECC.

The costs of LC3-ECC and OPC-ECC are similar regardless of the low cost of LC3 cement because fiber contributes to the main cost of ECC. The cost of LC3-PP-ECC was found to be only 39% of M45-ECC due to the coupled use of PP fiber and LC3 cement. Though the cost of LC3-ECC ($166/m^3) is higher than concrete ($108/m^3), LC3-ECC can still be competitive due to its ductility and durability advantages when reduced repair frequencies are accounted for.

The MSIs discussed above focus on analyzing sustainability at the ECC materials level. For a more precise sustainability metric, a life cycle assessment (LCA) model could be utilized. The LCA models based on OPC-ECC demonstrated significant advantages in environmental performance and materials cost over the lifecycle [7,64]. The most important source of energy and CO_2 savings are derived from the lowering traffic change, and the second is from a reduction of material usage associated with less frequent repair events. LC3-ECC has larger strain capacity, better self-healing ability, and is much greener than OPC-ECC. Although a complete LCA model of LC3-ECC is beyond the scope of this study, infrastructure using LC3-ECC is expected to have a longer service life and with fewer repair events, resulting in lower life-cycle embodied energy and carbon footprint.

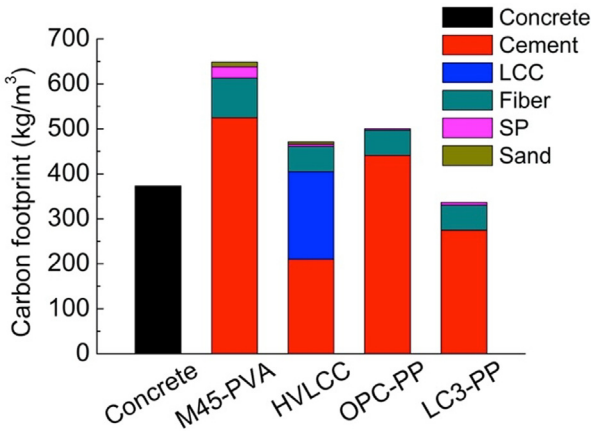

Fig. 13. The carbon footprint of LC3-ECC and other common materials.

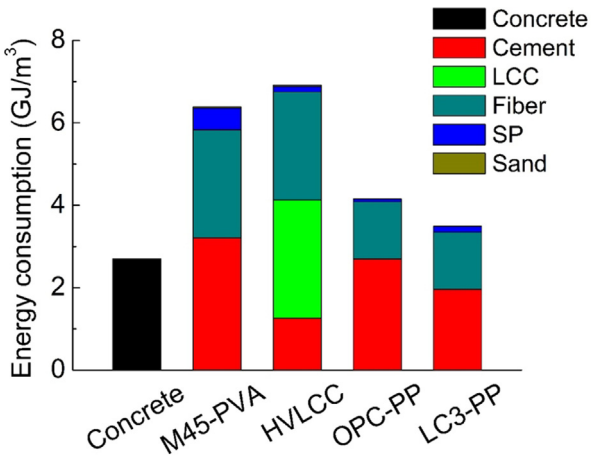

Fig. 14. Energy consumptions of LC3-ECC and other common materials.

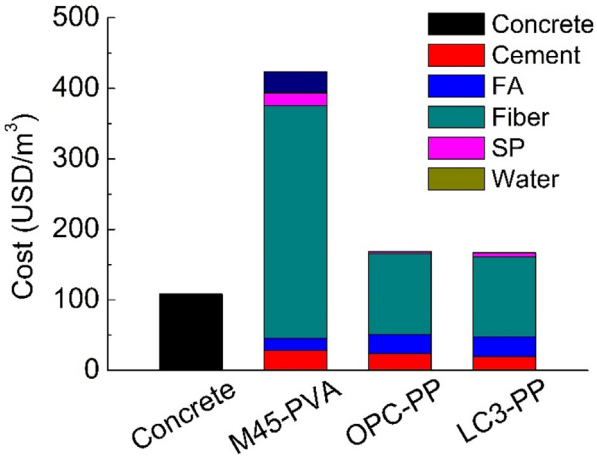

Fig. 15. Material costs of LC3-ECC and other common materials.

4. Conclusions

A sustainable ECC is developed using LC3 cement and PP fiber. The developed LC3-ECC is more ductile, more durable, greener, and less costly than OPC-ECC. Based on experimental tests and MSI calculations, the following conclusions can be drawn:

- The 28-day compressive strength of LC3-ECC (21–46 MPa) meets the requirements of common structural and non-structural applications. The high strain capacity (6–9%) makes it an attractive material for enhanced structural resilience.
- LC3-ECC has self-healing ability due to its tight crack width and large strain capacity despite the lower OPC content. These characteristics are expected to support structural durability in the field.
- LC3-ECC shows improved sustainability over previously studied ECC using OPC binder and PVA fiber. The carbon footprint of LC3-ECC is reduced to 52% of M45 and 90% of conventional concrete. The embodied energy of LC3-ECC is 55% of M45 ECC. Considering the significant advantages of good tensile performance and durability, LC3-ECC has a competitive material cost ($166/$m^3$) compared to M45 and concrete. Longer service life and fewer repair requirements further improve the sustainability of LC3-ECC for the whole life cycle of civil infrastructure.

CRediT authorship contribution statement

He Zhu: Conceptualization, Methodology, Investigation, Formal analysis, Writing - original draft. **Duo Zhang:** Formal analysis, Writing - review & editing. **Tianyu Wang:** Investigation. **Haoliang Wu:** Investigation. **Victor C. Li:** Funding acquisition, Project administration, Conceptualization, Writing - review & editing.

Declaration of Competing Interest

The authors declare that they have no known competing financial interests or personal relationships that could have appeared to influence the work reported in this paper.

Acknowledgments

This research is partially supported by an ARPA-e grant (DE-AR0001141) to the University of Michigan. Materials supply from BORAL RESOURCES (fly ash), BASF (water reducer), Omya (limestone), and Sika (metakaolin) is gratefully acknowledged.

References

[1] V.C. Li, Engineered Cementitious Composites (ECC): Bendable Concrete for Sustainable and Resilient Infrastructure, Springer, 2019.
[2] Y.C. Díaz, S.S. Berriel, U. Heierli, A.R. Favier, I.R.S. Machado, K.L. Scrivener, J.F.M. Hernández, G. Habert, Limestone calcined clay cement as a low-carbon solution to meet expanding cement demand in emerging economies, Dev. Eng. 2 (2017) 82–91.
[3] B. Felekoglu, K. Tosun-Felekoglu, R. Ranade, Q. Zhang, V.C. Li, Influence of matrix flowability, fiber mixing procedure, and curing conditions on the mechanical performance of HTPP-ECC, Compos. B Eng. 60 (2014) 359–370.
[4] E. Yang, S. Wang, Y. Yang, V.C. Li, Fiber-bridging constitutive law of engineered cementitious composites, J. Adv. Concr. Technol. 6 (2008) 181–193.
[5] L. Li, Z. Cai, K. Yu, Y.X. Zhang, Y. Ding, Performance-based design of all-grade strain hardening cementitious composites with compressive strengths from 40 MPa to 120 MPa, Cem. Concr. Compos. 97 (2019) 202–217.
[6] R. Ranade, Advanced Cementitious Composite Development for Resilient and Sustainable Infrastructure, University of Michigan, Ann Arbor, 2014, p. 419.
[7] H. Zhang, M.D. Lepech, G.A. Keoleian, S. Qian, V.C. Li, Dynamic life-cycle modeling of pavement overlay systems: capturing the impacts of users, construction, and roadway deterioration, J. Infrastruct Syst. 16 (2010) 299–309.
[8] V.C. Li, On engineered cementitious composites (ECC), J. Adv Concr Technol. 1 (2003) 215–230.
[9] M.D. Lepech, V.C. Li, R.E. Robertson, G.A. Keoleian, Design of green engineered cementitious composites for improved sustainability, Aci Mater. J. 105 (2008) 567.
[10] V.C. Li, M.D. Lepech, S. Wang, M. Weimann, G.A. Keoleian, Development of green ECC for sustainable infrastructure systems, (2004).
[11] K. Yu, Y. Wang, J. Yu, S. Xu, A strain-hardening cementitious composites with the tensile capacity up to 8%, Constr. Build. Mater. 137 (2017) 410–419.
[12] J. Zhou, S. Qian, M.G. Sierra Beltran, G. Ye, K. van Breugel, V.C. Li, Development of engineered cementitious composites with limestone powder and blast furnace slag, Mater. Struct. 43 (2010) 803–814.
[13] J. Yu, C.K.Y. Leung, Strength improvement of strain-hardening cementitious composites with ultrahigh-volume fly ash, J. Mater. Civil Eng. 29 (2017) 05017003.
[14] K. Scrivener, F. Martirena, S. Bishnoi, S. Maity, Calcined clay limestone cements (LC3), Cement Concrete Res. 114 (2018) 49–56.
[15] K.L. Scrivener, Options for the future of cement, Indian Concr. J. 88 (2014) 11–21.
[16] S.S. Berriel, A. Favier, E.R. Domínguez, I.R.S. Machado, U. Heierli, K. Scrivener, F. Martiren, Hernández, G. Habertd, Assessing the environmental and economic potential of Limestone Calcined Clay Cement in Cuba, J. Clean. Prod. 124 (2016) 361–369.
[17] B.H. Zaribaf, B. Uzal, K. Kurtis, Compatibility of Superplasticizers with Limestone-Metakaolin Blended Cementitious System, Calcined Clays for Sustainable Concrete, Springer, 2015, pp. 427–434.
[18] Y. Dhandapani, T. Sakthivel, M. Santhanam, R. Gettu, R.G. Pillai, Mechanical properties and durability performance of concretes with Limestone Calcined Clay Cement (LC3), Cem. Concr. Res. 107 (2018) 136–151.
[19] S. Karen, A. François, M. Hamed, Z. Franco, S. Julien, H. Wilasinee, F. Aurélie, Impacting factors and properties of limestone calcined clay cements (LC3), Green Mater. 7 (2019) 3–14.
[20] A.C. Emmanuel, P. Haldar, S. Maity, S. Bishnoi, Second pilot production of limestone calcined clay cement in India: the experience, Indian Concr. J. 90 (2016) 57–64.
[21] K. Turk, S. Demirhan, Effect of limestone powder on the rheological, mechanical and durability properties of ECC, Eur J. Environ. Civ. En. 21 (2017) 1151–1170.
[22] H. Siad, A. Alyousif, O.K. Keskin, S.B. Keskin, M. Lachemi, M. Sahmaran, K.M.A. Hossain, Influence of limestone powder on mechanical, physical and self-healing behavior of Engineered Cementitious Composites, Constr. Build. Mater. 99 (2015) 1–10.
[23] E. Gödek, K. Tosun Felekoğlu, M. Keskinateş, B. Felekoğlu, Development of flaw tolerant fiber reinforced cementitious composites with calcined kaolin, Appl. Clay Sci. 146 (2017) 423–431.
[24] B. Felekoğlu, K. Tosun-Felekoğlu, M. Keskinateş, E. Gödek, A comparative study on the compatibility of PVA and HTPP fibers with various cementitious matrices under flexural loads, Constr. Build. Mater. 121 (2016) 423–428.
[25] Y. Zheng, L.F. Zhang, L.P. Xia, Investigation of the behaviour of flexible and ductile ECC link slab reinforced with FRP, Constr. Build. Mater. 166 (2018) 694–711.
[26] E. Özbay, O. Karahan, M. Lachemi, K.M.A. Hossain, C.D. Atis, Investigation of properties of engineered cementitious composites incorporating high volumes of fly ash and metakaolin, Aci Mater. J. 109 (2012) 565–571.
[27] E. Yang, V.C. Li, Strain-hardening fiber cement optimization and component tailoring by means of a micromechanical model, Constr. Build. Mater. 24 (2010) 130–139.
[28] H.R. Pakravan, M. Jamshidi, M. Latifi, Study on fiber hybridization effect of engineered cementitious composites with low- and high-modulus polymeric fibers, Constr. Build. Mater. 112 (2016) 739–746.
[29] ASTM C150/C150M-20, Standard Specification for Portland Cement, ASTM International, West Conshohocken, PA, 2020.
[30] J. Camilleri, Characterization and hydration kinetics of tricalcium silicate cement for use as a dental biomaterial, Dent. Mater. 27 (2011) 836–844.
[31] A.M. Matos, L. Maia, S. Nunes, P. Milheiro-Oliveira, Design of self-compacting high-performance concrete: Study of mortar phase, Constr. Build. Mater. 167 (2018) 617–630.
[32] M. Benitez-Guerrero, J.M. Valverde, P.E. Sanchez-Jimenez, A. Perejon, L.A. Perez-Maqueda, Multicycle activity of natural CaCO3 minerals for thermochemical energy storage in Concentrated Solar Power plants, Sol. Energy. 153 (2017) 188–199.
[33] J. Yu, H. Wu, C.K.Y. Leung, Feasibility of using ultrahigh-volume limestone-calcined clay blend to develop sustainable medium-strength Engineered Cementitious Composites (ECC), J. Clean. Prod. 262 (2020) 121343.
[34] K. Yu, Y. Ding, J. Liu, Y. Bai, Energy dissipation characteristics of all-grade polyethylene fiber-reinforced engineered cementitious composites (PE-ECC), Cem. Concr. Compos. 106 (2020) 103459.
[35] ASTM C1437-15, Standard Test Method for Flow of Hydraulic Cement Mortar, ASTM International, West, Conshohocken, PA, 2015.
[36] ASTM C109/C109M-20a, Standard Test Method for Compressive Strength of Hydraulic Cement Mortars (Using 2-in. or [50-mm] Cube Specimens), ASTM International, West Conshohocken, PA, 2020.
[37] H. Wu, D. Zhang, B.R. Ellis, V.C. Li, Development of reactive MgO-based Engineered Cementitious Composite (ECC) through accelerated carbonation curing, Constr. Build. Mater. 191 (2018) 23–31.
[38] K. Yu, Z. Lu, J. Dai, S.P. Shah, Direct tensile properties and stress-strain model of UHP-ECC, J. Mater. Civil Eng. 32 (2020) 04019334.

[39] V.C. Li, E. Yang, Self Healing in Concrete Materials, Self Healing Materials, Springer, 2007, pp. 161–193.
[40] Y. Yang, E. Yang, V.C. Li, Autogenous healing of engineered cementitious composites at early age, Cem. Concr. Res. 41 (2011) 176–183.
[41] W. Li, B. Dong, Z. Yang, J. Xu, Q. Chen, H. Li, F. Xing, Z. Jiang, Recent advances in intrinsic self-healing cementitious materials, Adv. Mater. 30 (2018) 1705679.
[42] ASTM C215-19, Standard Test Method for Fundamental Transverse, Longitudinal, and Torsional Resonant Frequencies of Concrete Specimens, ASTM International, West Conshohocken, PA, 2019.
[43] F. Avet, K. Scrivener, Investigation of the calcined kaolinite content on the hydration of Limestone Calcined Clay Cement (LC3), Cem. Concr. Res. 107 (2018) 124–135.
[44] V. Bonavetti, H. Donza, G. Menéndez, O. Cabrera, E.F. Irassar, Limestone filler cement in low w/c concrete: a rational use of energy, Cem. Concr. Res. 33 (2003) 865–871.
[45] M. Antoni, J. Rossen, F. Martirena, K. Scrivener, Cement substitution by a combination of metakaolin and limestone, Cem. Concr. Res. 42 (2012) 1579–1589.
[46] R. Trauchessec, J.M. Mechling, A. Lecomte, A. Roux, B. Le Rolland, Hydration of ordinary Portland cement and calcium sulfoaluminate cement blends, Cem. Concr. Compos. 56 (2015) 106–114.
[47] F. Deschner, F. Winnefeld, B. Lothenbach, S. Seufert, P. Schwesig, S. Dittrich, F. Goetz-Neunhoeffer, J. Neubauer, Hydration of Portland cement with high replacement by siliceous fly ash, Cem. Concr. Res. 42 (2012) 1389–1400.
[48] M. Li, V.C. Li, Rheology, fiber dispersion, and robust properties of Engineered Cementitious Composites, Mater. Struct. 46 (2013) 405–420.
[49] F. Nazário Santos, S. Raquel Gomes De Sousa, A. José Faria Bombard, S. Lopes Vieira, Rheological study of cement paste with metakaolin and/or limestone filler using Mixture Design of Experiments, Constr. Build. Mater. 143 (2017) 92–103.
[50] Q. Zhang, V.C. Li, Development of durable spray-applied fire-resistive engineered cementitious composites (SFR-ECC), Cem. Concr. Compos. 60 (2015) 10–16.
[51] H. Nguyen, P. Kinnunen, V. Carvelli, M. Mastali, M. Illikainen, Strain hardening polypropylene fiber reinforced composite from hydrated ladle slag and gypsum, Compos. B Eng. 158 (2019) 328–338.
[52] B. de LHONEUX, R. Kalbskopf, P. Kim, V.C. Li, Z. Lin, D. Vidts, S. Wang, H. Wu, Development of high tenacity polypropylene fibers for cementitious composites, (2002).
[53] K. Tosun-Felekoğlu, E. Gödek, M. Keskinateş, B. Felekoğlu, Utilization and selection of proper fly ash in cost effective green HTPP-ECC design, J. Clean. Prod. 149 (2017) 557–568.
[54] S. Deb, N. Mitra, S.B. Majumder, S. Maitra, Improvement in tensile and flexural ductility with the addition of different types of polypropylene fibers in cementitious composites, Constr. Build. Mater. 180 (2018) 405–411.
[55] F. Li, Z. Feng, K. Deng, Y. Yu, Z. Hu, H. Jin, Axial behavior of reinforced PP-ECC column and hybrid NSC-ECC column under compression, Eng. Struct. 195 (2019) 223–230.
[56] M.D. Lepech, A Paradigm for Integrated Structures and Materials Design for Sustainable Transportation Infrastructure, University of Michigan, Ann Arbor, 2006.
[57] W. Zhang, C. Yin, F. Ma, Z. Huang, Mechanical properties and carbonation durability of engineered cementitious composites reinforced by polypropylene and hydrophilic polyvinyl alcohol fibers, Materials 11 (2018) 1147.
[58] V.C. Li, E. Herbert, Robust self-healing concrete for sustainable infrastructure, J. Adv. Concr. Technol. 10 (2012) 207–218.
[59] L. Kan, H. Shi, Investigation of self-healing behavior of engineered cementitious composites (ECC) materials, Constr. Build. Mater. 29 (2012) 348–356.
[60] Z. Zhang, Q. Zhang, V.C. Li, Multiple-scale investigations on self-healing induced mechanical property recovery of ECC, Cem. Concr. Compos. 103 (2019) 293–302.
[61] A. Klemm, D. Wiggins, 12 – Sustainability of natural stone as a construction material, Sustainability of Construction Materials (Second Edition), Woodhead Publishing, 2016. pp. 283–308.
[62] L. Čuček, J.J. Klemeš, Z. Kravanja, Chapter 5 – Overview of Environmental Footprints, Assessing and Measuring Environmental Impact and Sustainability, Butterworth-Heinemann, Oxford, 2015, pp. 131–193.
[63] Y.S. Song, J.R. Youn, T.G. Gutowski, Life cycle energy analysis of fiber-reinforced composites, Compos. A Appl. Sci. Manuf. 40 (2009) 1257–1265.
[64] G.A. Keoleian, A. Kendall, J.E. Dettling, V.M. Smith, R.F. Chandler, M.D. Lepech, V.C. Li, Life cycle modeling of concrete bridge design: comparison of engineered cementitious composite link slabs and conventional steel expansion joints, J. Infrastruct Syst. 11 (2005) 51–60.